Earthquake Engineering, Tenth World Conference © 1992 Balkema, Rotterdam. ISBN 90 5410 060 5

Use of experimental data to develop probable behavior for structural components

W.K. Hong
Samsung Engineering & Construction Co., Ltd, Seoul, Korea

G.C. Hart
University of California, Los Angeles, Calif., USA

ABSTRACT: The primary objective of earthquake structural engineering research is to ensure the safety of structures by understanding and improving a design methodolgy. Ideally, this would require the development of an analytical model related to a design methodolgy that insures a ductile performance. For the accurate assessment of the adequacy of an analytically developed structural model, experiments conducted to study the inplane inelastic cyclic behavior of structures should verify the analytical approach. The fundamental goal of this paper is to present and demonstrate experimentally verified analytical methods that provide the adequate degree of safety and confidence in the behavior of reinforced concrete structural components. This study further attempts to extend the developed modeling technique for use by practicing structural engineers for both the analysis and design.

1 INTRODUCTION

When a structure is loaded at its near-maximum capacity it should be capable of demonstrating enough toughness or ductility to undergo the deformation required to avoid brittle and catastrophic failure. Extensive attention has been paid to clarify the flexural failure mechanisms to the extend that well understood conclusions incorporated into design concept have been drawn.

Structures in general evolve through several identifiable states of behavior until they fail. Cracking limit state, yield limit state, and the maximum load limit state have been considered as the key limit states in this paper. This paper attempts to analytically identify the behavior states and the limit states of structural components based on stress strain curve of both confined and unconfined concrete structures. Computer program developed can perform inelastic analysis of structural components based upon a stress strain curve provided by the user or the Kent-Park stress strain curve as modified in this paper. The optional analyses include an interaction diagram and a moment curvature diagram. The system displacement ductility is also calculated to see how ductile structures under consideration are. Strain hardening in reinforcing steel may be allowed.

Sixteen story height reinforced concrete masonry shear walls have been tested and the sensitivity of response is studied to various design parameters and the load conditions, such as amount of vertical and horizontal reinforcement and the applied axial stress. Experimental data obtained in the test have been compared to the analytical data, indicating the accuracy of the analytical model.

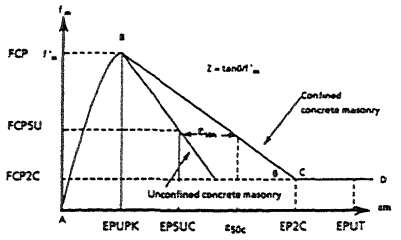

Fig. 1 Stress-strain curve for confined and unconfined concrete masonry after kent and park(1).

2 ANALYTICAL MODELING OF THE CAPACITY OF STRUCTURAL COMPONENTS

2.1 Modified Kent-Park stress strain curve

Figure 1 depicts a typical stress strain curve for confined and unconfined concrete after Kent and Park the parameters of which the user may specify. In this study parameters that constitute the Kent-Park stress strain curve have been identified for the shear structures through database collected from the 2 wall experimental study. Users may use their stress strain curves upon which the calculation of the mean stress factor, α, and the centroid factor, γ, is made.

2.2 Structural mechanics

Equations (1) and (2) show the equilibrium equations for the concrete section with both

compression and tension reinforcement and Equation (3) represents the curvature at a given strain level. Mean stress factor, α, and centroid factor, γ, are also provided in Equations (5) and (6).

$$P = \alpha f''_c bkd + \Sigma f_{si} A_{si} \quad (1)$$

$$M = \alpha f''_c bkd(d - \gamma kd) + \Sigma f_{si}A_{si}(d - d_i) - P_e \quad (2)$$

$$\phi = \varepsilon_{cm}/kd \quad (3)$$

$$e = \frac{\{0.85f'_c bL_w(d-L_w/2) + A_s' f_y(d-d')\}}{\{0.85f'_c bL_w+(A_s+A_s')f_y\}} \quad (4)$$

$$\alpha = \frac{\int_0^{\varepsilon_{cm}} f_c d\varepsilon_c}{f''\varepsilon_{cm}} \quad (5)$$

$$\gamma = 1 - \frac{\int_0^{\varepsilon_{cm}} \varepsilon_c f_c d\varepsilon_c}{\varepsilon_{cm}\int_0^{\varepsilon_{cm}} f_c d\varepsilon_c} \quad (6)$$

Equation (4) indicates the distance from the plastic centroid to the centroid of the tension steel of the section. To generate the moment curvature relationship moment capacity is calculated for each strain level allowed to increase to the maximum strain level that structures may resist. For each strain level iteration technique is employed to adopt the location of neutral axis, kd, which satisfies the internal force equilibrium equation. Then next step is to calculate stress level of the reinforcing steels. Three cases of steel layers are considered in this study. In case 1 the bars are only distributed uniformly around four faces. All faces must have the same number of bars. Total number of bars must always be an integer multiple of four. Case 2 has the bars at layers distributed uniformly over the depth. Each layer must have at least two bars. All bars in the same layer are of the same size. Total number of layers must be at least two. In Case 3 the bar groups (one, two or more bars in a group) are located in any desired position.

2.3 Modeling of confined concrete

For a confined concrete at large strains it is possible that the unconfined concrete outside the ties (i.e. the cover concrete) may spall away. It is assumed that the cover concrete follows the same stress strain curve as the confined core up to the strain of EPCR, but carries no stress at higer strains. For confined concrete at every strain level the procedure developed in this study checks for spalling of concrete cover. If the concrete cover spalls away then only the area of concrete confined by confining steel is used in the analysis. For confined concrete the developed procedure calculates the required area of confining steel to allow the strain EPUT, or EP5UC in the case of a user defined curve, in the concrete. The modified mathematical expression of *falling branch after the peak stress was proposed* by this study to account for the strength degradation as observed in the expriments and shown in Equation (2).

2.4 Mathematical modeling of strain hardening of steel

At large strains it is possible that the reinforcing steel may experience the strain hardening. The actual shape of the steel stress strain curve must be considered to obtain an accurate estimate of the moment and curvature. Figure 3 shows the general shape of the steel stress strain curve.

2.5 Assessment of displacement ductility

The lateral deflection at the top of the cantilever wall due to concentrated load applied at the end (Figure 2) is determined by taking moments of the curvature diagram about the top (free end).

For uniformly distributed load across the number length, ductility has been calculated as follows

$$\text{Ductility} = 1 + [4.0/A_e(\phi u/\phi y - 1)(1-1/2A_e) \quad (7)$$

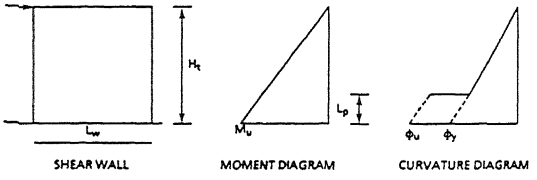

Fig. 2 Cantilever wall with lateral loading at ultimate.

2.6 Limit stress and analytical prediction of each limit state

2.6.1 Cracking limit state

The uncracked section behavior state corresponds to the stress level at which the load induced tensile stress at the extreme tension fiber is less than the modulus of rupture defined by Equation (8). Therefore the cross section is uncracked and the load induced moment is less than the cracking moment capacity calculated by Equation (9).

$$f_r = 4.0\sqrt{f'_c} \quad (8)$$

$$M_{cr} = [(P/A) + f_r]S \quad \text{where } S = bd^2/6 \quad (9)$$

The cracked section limit state exists when the

load induced moment is equal to the cracking moment of the cross section.

2.6.2 Yield limit state

In this behavior states the section is cracked with the strain in the steel less than its yield strain. The load induced moment is greater than the cracking moment capacity but less than the yield moment capacity. The yield limit state exists when the strain in the steel equals to the yield strain.

2.6.3 Maximum load limit state

At the next behavior state, the section is cracked with strain in the steel greater than its yield strain, but the maximum strain at the extreme compression fiber in concrete is less than its ultimate maximum usable strain. The maximum load limit state exists when the strain at the extreme fiber is equal to the maximum usable strain.

3 EXPERIMENTAL DATA AND DEVELOPMENT PROBABLE BEHAVIOR OF STRUCTURAL COMPONENT BASED ON TEST DATA

3.1 Test set up

The objective of this experiment was to evaluate the inelastic load resistance mechanism and the failure mode of story height reinforced concrete masonry shear walls. The wall panels were subjected to inplane lateral and axial loads which simulate seismic and bearing loads exerted on a wall situated in reinforced concrete masonry building. Sixteen story height reinforced concrete masonry shear walls have been tested and Table 1 shows the information of the axial stress, the vertical and horizontal reinforcement. Tables 2 and 3 present the same information, rearranged to better illustrate axial load/vertical and axial load/horizontal rebar combinations. A total of sixteen reinforced concrete masonry shear wall specimen has been tested.

Table 1. Axial load and steel variables.

Wall	Axial Load (psi)	Vertical Steel	Horizontal Steel
1	200	5 x #5	5 x #4
2	270	5 x #5	9 x #3
3	270	5 x #7	5 x #3
4	0	5 x #7	5 x #3
5	100	5 x #7	5 x #3
6	0	5 x #5	5 x #3
7	100	5 x #7	5 x #3
8	0	5 x #5	5 x #4
9	270	5 x #5	5 x #3
10	100	5 x #5	5 x #3
11	0	5 x #7	5 x #4
12	100	5 x #5	5 x #4
13	270	5 x #6	5 x #4
14	270	5 x #6	5 x #3
15	100	5 x #6	5 x #4
16	270	5 x #7	5 x #4

Table 2. Test matrix/horizontal steel.

	Axial Load 0 psi		Axial Load 100 psi		Axial Load 200 psi		Axial Load 270 psi	
	Wall	Vertical Steel	Wall	Vertical Steel	Wall	Vertical Steel	Wall	Vertical Steel
Horizontal Steel 5 x #3	4	5 x #7	5	5 x #7			3	5 x #7
	6	5 x #5	7	5 x #7			9	5 x #5
			10	5 x #5			14	5 x #6
Horizontal Steel 5 x #4	8	5 x #5	12	5 x #5	1	5 x #5	13	5 x #6
	11	5 x #7	15	5 x #6			16	5 x #7
Horizontal Steel 9 x #3							2	5 x #5

1 ksi = 6.895 MPa

Table 3. Test matrix/vertical steel.

	Axial Load 0 psi		Axial Load 100 psi		Axial Load 200 psi		Axial Load 270 psi	
	Wall	Horizontal Steel	Wall	Horizontal Steel	Wall	Horizontal Steel	Wall	Horizontal Steel
Vertical Steel 5 x #5	6	5 x #3	10	5 x #3	1	5 x #4	2	9 x #3
	8	5 x #4	12	5 x #4			9	5 x #3
Vertical Steel 5 x #6			15	5 x #4			13	5 x #4
							14	5 x #3
Vertical Steel 5 x #7	4	5 x #3	5	5 x #3			3	5 x #3
	11	5 x #4	7	5 x #3			16	5 x #4

1 ksi = 6.895 MPa

As shown in Figure 3 the specimen were 6 ft high and 6 ft long and fabricated with a single wythe of 6x8x16 hollow concrete blocks. They were fully grouted with uniformly distributed vertical and horizontal reinforcement. The horizontal reinforcement had 180 degree hooks around the extreme vertical steel. Each specimen had a reinforced concrete top beam and base slab. The vertical reinforcement ran continuously from the base slab to the top beam with 180 degree anchoring hooks. Bond-beam units were used throughout the wall panel to allow the placement of horizontal reinforcement and enhance the continuity of the grout. The construction of a typical specimen is shown in Figure 3 and the test set up is shown in Figure 4.

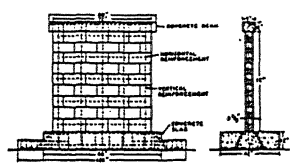

Fig. 3 Test specmen.

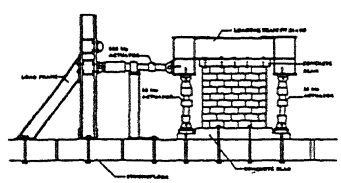

Fig. 4 Test setup.

Several design parameters and loading conditions were investigated and the influence of the axial load, the reinforcement ratios and the lateral

load history on the failure mode of the walls were examined in this experiment. These included magnitude of the axial load, the reinforcement ratio in the vertical as well as the horizontal direction, and the history of the laterally applied load. Each of sixteen specimen was loaded while the magnitude of the axial load was maintained constant during test. The experiments were performed using a load controlled technique until the vertical steel yielded and then followed by a displacements controlled technique. Automatic data acquisition system installed with specimen points out the level of lateral force which causes the vertical reinforcing steel to yield and the limit state associated with this force level is referred as a yield limit state. The maximum load limit state can also be identified when the wall specimen is in the vicinity of its ultimate load capacity.

3.2 Parameters used in analytical model

The experimental values for the yield stress of steel and the strain of unconfined masonry at maximum compressive stress were used to analytically calculate the values of moment capacity for each limit state in the mathematical model. The modified Kent-Park stress strain curve with parameters identified from tested shear walls was used in the model. The strain at maximum stress was set at 0.002, while the maximum usable strain for unconfied masonry was set at 0.003.

The height of the shear wall is 6 ft and height of the plastic hinge region is assumed to be 30 percent of the wall height.

4 COMPARISON

4.1 Ductile failure mode

Table 4 shows the calculated limit state lateral loads in two sets of units. Those in KIPS correspond to the total lateral load. When the load is divided by the total cross sectional area of the wall it is denoted in PSI units. Walls with shear/flexural ratios great than 1.0 in Table 4 are hereinafter referred to as FLEXURAL WALLS. A flexural wall is a wall that has shear strength that exceeds its flexural strength calculated using Equation in Section 2412 of the 1988 UBC. These walls are expected to have the vertical flexural steel yield prior to the shear failure. In the last two columns of Table 4 both the analytical and observed failure modes are presented, demonstrating an excellent agreement between two observations.

4.2 Definition of virgin and stabilized cycles

The experiments were conducted with static cyclic load reversals. The first time the drift extends into a new and larger amplitude of drift domain it is called a virgin loading cycle. After this cycle, the subsequent cycles are repeated with drift being the same until the force has stabilized. For example, Figure 5 shows a plot of cycles 25, 26, and 27 with the first being the virgin cycle and the last being the stabilized cycle.

Table 4. Calculated limit state lateral loads.

Wall No.	Flexural Cracking		Flexural Yield		Flexural Strength	
	V_{cr} (kips)	V_{cr} (psi)	V_y (kips)	V_y (psi)	Y_{max} (kips)	V_{max} (psi)
1	28	64	59	136	72	168
2	33	115	69	493	81	187
3	33	76	99	230	118	273
4	16	37	64	147	91	211
5	23	52	77	179	103	239
6	16	37	32	73	46	106
7	24	56	79	182	107	247
8	18	41	31	72	46	106
9	36	83	72	166	87	202
10	24	56	47	108	61	144
11	18	41	65	149	91	213
12	24	56	47	108	63	145
13	36	83	84	194	105	242
14	36	83	84	194	105	242
15	25	57	60	139	82	189
16	34	78	98	227	120	278

Wall No.	Shear		Shear/ Flexure	Failure Mode	
	V_{sh} (kips)	V_{sh} (psi)		Analytical	Test
1	80	185	1.1	flexure	flexure
2	86	199	1.1	flexure	flexure
3	59	137	0.5	shear	shear
4	60	139	0.7	shear	shear
5	60	139	0.6	shear	shear
6	57	132	1.2	flexure	flexure/slide
7	63	146	0.6	shear	shear
8	85	197	1.9	flexure	flexure/slide
9	59	137	0.7	shear	shear
10	60	137	1.0	flexure	flexure/shear
11	90	208	1.0	flexure	shear/slide
12	85	197	1.4	flexure	flexure
13	87	201	0.8	shear	shear
14	60	139	0.6	shear	shear
15	87	201	1.1	flexure	flexure/shear
16	87	201	0.7	shear	shear

1 kip = 4.448 kN, 1 ksi = 6.895 MPa

4.3 Comparison between calcuated and experimental limit state values

Tables 5, 6, and 7 compare the analytical value at yield limit state and maximum load limit state to the experimental data obtained at the same limit states. The ratio of the experimental data to the analytical values for the yield limit state is calculated in Table 5 for flexural shear walls. The mean and the coefficient of variation of this ratio are 1.13 and 2.1 %, respectively. The ratio of the minimum measured maximum load experimental data to the analytical values for the maximum load limit state are given in Table 6 and they indicate that the analytical prediction compares well with the experimental data. Table 7 presents a more indepth comparison of the measured maximum lateral load and the calculated load. The columns denoted (min/calc) are ratios of minimum virgin and minimum stabilized lateral loads to the calculated loads. For example, since the experimental data was available for the virgin tests the ratio of minimum virgin load (in this case the negative value of 78 kips) is divided by the calculated

Table 5. Calculated and measured flexural yield limit state values

Wall	Calculated (kips)	Measured (kips)*	(Measured/ Calculated)
1	59	60	1.02
2	69	76	1.10
6	32	40	1.25
8	31	36	1.16
10	47	NA**	NA
11	65	NA	NA
12	47	NA	NA
15	60	NA	NA

* Measured values are from a virgin loading curve and correspond to first yield as measured using a strain gauge on a reinforcing bar.
** NA = Not available due to strain gauge malfunction.

1 kip = 4.448 kN

Table 6. Calculated and measured flexural strength limit state values.

Wall	Calculated (kips)	Measured (kips)*		(Minimum Measured/ Calculated)
		Positive	Negative	
1	72	+87	-78	1.08
2	81	+83	-98	1.02
6	46	+52	-47	1.02
8	46	+50	-47	1.02
10	60	+69	-67	1.12
11	90	+89	-95	0.99
12	63	+71	-71	1.13
15	82	+82	-94	1.00

* Measured values are from virgin load deflection curves.

1 kip = 4.448 kN

Table 7. Calculated and measured flexural strength limit state values.

Wall	Min/Calc		Max/Calc		Ave/Calc	
	Virgin	Stblzd	Virgin	Stblzd	Virgin	Stblzd
1	1.08	0.86	1.21	1.07	1.15	0.97
2	1.02	0.93	1.21	1.07	1.12	1.00
6	1.04	0.93	1.13	0.96	1.09	0.95
8	1.02	0.91	1.09	0.96	1.05	0.93
10	1.12	0.97	1.15	1.05	1.13	1.01
11	0.99	0.89	1.06	0.94	1.02	0.92
12	1.13	1.02	1.13	1.03	1.13	1.02
15	1.00	0.88	1.15	1.05	1.07	0.96
Mean	1.05	0.92	1.14	1.02	1.10	0.97
Cov (%)	4.7	5.1	4.4	5.0	3.7	2.6

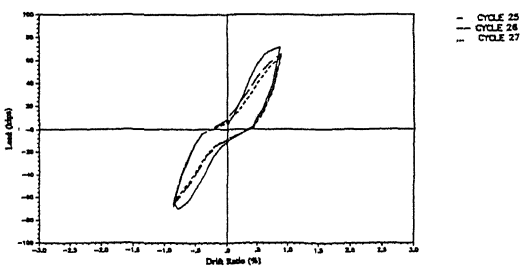

Fig. 5 Cycles 25, 26 and 27.

value to obtain the ratio of 1.08 for Wall #1 in Table 7. Because the stabilized load is always less than the corresponding virgin peak (i.e., the cracking due to cyclic loading reduces the strength for a given drift), it follows that its ratio (0.86 in this case) is less than 1.08. The eight walls had an average value of 1.05 for the minimum virgin test data and 0.92 for the minimum stabilized test data. The coefficients of variation were 4.7 and 5.1 %, repectively. The columns in Table 7 denoted as (max/calc) correspond to the positive measured value if the minimum peak was negative as it was in Wall #1. A comparison of Tables 6 and 7 reveals in what cases the minimum is positive. In the test program the direction is considered positive in which the load or drift was always increased into a new domain for the first time. The eight walls had an average of 1.14 for the maximum virgin test data and 1.02 for the maximum stabilized test data. The corresponding coefficient of variation values were 4.4 and 5.0 %, respectively. The columns in Table 7 marked (ave/calc) are obtained by averaging the minimum and the maximum ratios. For example, (1.08+1.21)/2 is equal to 1.15. If these values are compared for all 8 walls, the virgin and stabilized mean values become 1.10 and 0.97, repectively.

The ratio of the maximum load limit state values to the yield limit state values for the analytical predictions is calculated and shown in Table 8. Also the ratio of the maximum virgin load limit state to the yield limit state for the experimental data is shown in this table. For example, the mean and the coefficient of variation of the ratio for the analytical prediction are 1.34 and 7.4 %, whereas those of the experimental data are 1.36 and 6.6 % for the maximum test data and 1.22 and 9.1 for the minimum test data. It is noted that the mean and the coefficient of variation of the ratio of the maximum load moment capacity to the yield moment capcity for the analytical prediction are well compared to those of the experimental data as can be seen in Table 9. Upon the successful analytical calculation of the yield limit state the maximum load limit state value is then obtained by multiplying it by 1.34. This approach of calculating the maximum load limit state from the yield limit state demonstrates the simplicity with resonable accuracy that can be utilized by the practicing structural engineer. It is also interesting to calculate the mean and the coefficent of variation of the ratio of the analytical yield limit state to the analytical cracking limit state for each wall. The results are summarized in Table 9. It is noted that this ratio exceeds the recommended minimum ratio of 1.8 that is given in the 1989 amended version of the 1988 UBC. Table 10 summarizes results that include the shear stress and the neutral axis location of each limit state for the flexural walls. The shear stresses on net area for each limit state are calculated by dividing the lateral shear force by the total (i.e., gross) cross sectional area of the wall. Alternatively if the lateral shear is divided by the area of the wall in compression at the compression toe of the wall then the shear stresses on compression area is obtained. In the same table the neutral axis locations are also displayed for each limit state in the units of

Table 8. Calculated and measured ratio of maximum moment capacity to yield moment capacity.

Wall	Calculated Maximum/Yield Moment Capacity	Measured Maximum/Yield Moment Capacity	
		Maximum	Minimum
1	1.22	1.45	1.30
2	1.17	1.29	1.09
6	1.44	1.30	1.18
8	1.48	1.39	1.31
10	1.28	NA	NA
11	1.38	NA	NA
12	1.34	NA	NA
15	1.37	NA	NA
Mean	1.34	1.36	1.22
Cov (%)	7.4	6.6	9.1

Table 9. Calculated ratio of yield moment capacity to cracking moment capacity.

Wall #	M_y/M_{cr}
1	2.11
2	2.10
6	2.00
8	1.72
10	1.96
11	3.60
12	1.96
15	2.40
Mean	2.23
Cov (%)	24.0

Table 10. Lateral load at limit states.

Colorado FLEXURAL WALLS	Limit State	Lateral Force (kips)	Moment (K-Ft.)	Shear Stress (Psi)		Neutral Axis Location	
				on Net Area	on Comp. Area	Comp. Depth (In.)	% of the Wall Length
Wall #1	Cracking	27.7	166.0	64.0	114.7	40.2	56
	Yield	58.7	351.9	135.8	452.5	21.6	30
	Maximum	72.4	434.3	176.6	788.5	15.3	21
Wall #2	Cracking	32.5	195.0	75.2	114.5	47.3	66
	Yield	68.6	411.3	158.7	492.5	23.2	32
	Maximum	80.6	483.3	186.5	741.7	18.1	25
Wall #6	Cracking	15.8	95.0	36.7	207.8	12.7	18
	Yield	31.7	189.9	73.3	418.7	12.6	18
	Maximum	45.7	274.3	105.8	1120.5	6.8	9
Wall #8	Cracking	17.7	106.0	40.9	253.8	11.6	16
	Yield	31.0	186.1	71.8	449.5	11.5	16
	Maximum	45.8	274.9	106.1	1339.7	5.7	8
Wall #10	Cracking	24.2	145.0	55.9	183.9	21.9	30
	Yield	46.8	280.9	108.4	506.7	15.4	21
	Maximum	62.8	376.9	145.4	1246.4	8.4	12
Wall #11	Cracking	17.7	106.0	40.9	192.4	15.3	21
	Yield	64.5	386.9	149.3	702.4	15.3	21
	Maximum	92.8	556.8	214.8	1406.1	11.0	15
Wall #12	Cracking	24.2	145.0	55.9	183.9	21.9	30
	Yield	46.7	280.3	108.1	505.6	15.4	21
	Maximum	62.6	375.7	144.9	1242.4	8.4	12
Wall #15	Cracking	24.5	147.0	56.7	171.6	23.8	33
	Yield	60.1	360.8	139.2	614.9	16.3	23
	Maximum	81.8	490.8	189.4	1323.6	10.3	14

1 kip = 4.448 kN, 1 in. = 2.54 cm, 1 ksi = 6.895 MPa

inches and compression zone is obtained in terms of percentile of the wall length.

5 CONCLUSION

A well designed structure demonstrates a ductility necessary to undergo the deformation required to prevent sudden and premature failure before it collapses. The behavior and the limit states characterizing the performance of the structure were investigated to develop an appropriate analytical model related to design methodology that ensures the safety of structures. The analytical model proposed with modified version of Kent-Park stress starin curve to predict the behavior of the concrete structural components was validated by the experimental data, proving the accuracy of the model and its versatility. For the flexural shear walls whose shear capacity is greater than the flexural capacity ensuring the yield of vertical steel prior to the failure of the section excellent correlation between the analytical and observed test data has been achieved and this will bring reasonable means with easer access, allowing practicing engineers to confidently evaluate the capacity of concrete structural components to treat technical problems. In addition, the limit state design methodology may be reflected into the general engineering practice with extended degree of safety and confidence due to the analytical identification of the ultimate limit state. Finally the computation of deflection and ductility factor is also possible, and this will assist to prevent engineers from designing brittle structures not capable of resisting enough deformation required to ensure safe structures.

REFERENCES

Hart, G. C., Englekirk, R.E., and Hong, W. K.1987. "Structural Component Model of Flexural Walls", Proceedings of Fourth Meeting of the Joint Technical Coordinating Committee on Masonry Research U.S.- JAPAN Coordinated Earthquake Research Program", San Diego, California.

Priestly, M.J.N. 1981 "Ductility of Unconfined Masonry Shear Walls",Bullitin of the New Zealand National Society for Earthquake Engineering, Vol.14, NO.1.

Shing,P.B., Noland, J.L.,Spaeh,H.,and Klamerus, E. 1987. "Inelastic behavior of Masonry Wall panels Under In-Plane Cycle Loads", Proceedings of the Fourth North American Masonry Conference, Los Angeles, California.